Hydrogen sulfide-linked sulfhydration of NF-κB mediates its anti-apoptotic actions

Nilkantha Sen[1], **Bindu D. Paul**[1], **Moataz M. Gadalla**[4], **Asif K. Mustafa**[1], **Tanusree Sen**[3], **Risheng Xu**[1], **Seyun Kim**[1], and **Solomon H. Snyder**[1,2,*]

[1]The Solomon H. Snyder Department of Neuroscience, Johns Hopkins University School of Medicine, Baltimore, MD 21205, USA

[2]Departments of Pharmacology and Molecular Sciences, and Psychiatry, Johns Hopkins University School of Medicine, Baltimore, MD 21205, USA

[3]Department of Ophthalmology, Johns Hopkins University School of Medicine, Baltimore, MD 21205, USA

[4]Department of Pharmacology and Molecular Sciences, Johns Hopkins University School of Medicine, Baltimore, MD 21205, USA

Summary

Nuclear factor κB (NF-κB) is an anti-apoptotic transcription factor. We show that the anti-apoptotic actions of NF-κB are mediated by hydrogen sulfide (H_2S) synthesized by cystathionine gamma-lyase (CSE). TNFα treatment triples H_2S generation by stimulating binding of SP1 to the CSE promoter. H_2S generated by CSE stimulates DNA binding and gene activation of NF-κB, processes that are abolished in CSE deleted mice. As CSE deletion leads to decreased glutathione levels, resultant oxidative stress may contribute to alterations in CSE mutant mice. H_2S acts by sulfhydrating the p65 subunit of NF-κB at cysteine-38, which promotes its binding to the co-activator ribosomal protein S3 (RPS3). Sulfhydration of p65 predominates early following TNFα treatment, then declines and is succeeded by a reciprocal enhancement of p65 nitrosylation. Anti-apoptotic influences of NF-κB, which are markedly diminished in CSE mutant mice. Thus, sulfhydration of NF-κB appears to be a physiologic determinant of its anti-apoptotic transcriptional activity.

Introduction

The NF-κB family of transcription factors is stimulated by diverse agents including the multifunctional pro-inflammatory cytokine, tumor necrosis factor alpha (TNF-α), which activates the IκB kinase (IKK) complex that phosphorylates IκB proteins, leading to IκB degradation and NF-κB translocation to the nucleus (Delhase et al., 1999; Karin and Ben-Neriah, 2000). Nuclear functions of NF-κB are regulated by numerous substances including the ribosomal protein S3 (RPS3) (Wan et al., 2007).

Mice lacking the p65 subunit of NF-κB die at embryonic day 15 as a result of extensive liver apoptosis (Beg et al., 1995). Mouse embryonic fibroblasts (MEFs) lacking p65 are more

sensitive to TNF-α mediated cell death (Beg and Baltimore, 1996), indicating that NF-κB physiologically suppresses TNF-α mediated cell death. NF-κB induces the expression of several anti-apoptotic genes encoding substances such as cellular inhibitor of apoptosis (c-IAP), caspase-8–c-FLIP (FLICE inhibitory protein), A1 (also known as Bfl1), TNFR-associated factor 1 (TRAF1) and TRAF2 (Thuret et al., 1996).

Hydrogen sulfide (H_2S) is a physiologic messenger molecule involved in inflammation, suggesting a relationship to NF-κB. H_2S is generated in the periphery by cystathionine γ-lyase (cystathionase; CSE), while in the brain its biosynthesis may involve cystathionine β-synthase (CBS) (Kimura, 2010; Szabo, 2007). In mice with targeted deletion with CSE, H_2S formation is abolished in peripheral tissues. CSE knockout mice ($CSE^{-/-}$) display hypertension and a major decrease in endothelial derived relaxed factor activity, establishing H_2S as an important vasorelaxant (Szabo, 2007; Yang et al., 2008).

H_2S appears to signal predominantly by sulfhydrating cysteines of its target proteins such as GAPDH and actin which leads to augmentation of GAPDH catalytic activity and actin polymerization (Mustafa et al., 2009a; Mustafa et al., 2009b) thereby altering functions of a wide range of cellular proteins and enzymes (Li et al., 2011).

In the present study we show that TNF-α stimulates the transcription of CSE, and the generated H_2S sulfhydrates cysteine-38 of p65, enhancing its binding to the coactivator RPS3, thereby augmenting binding to the promoters of several anti-apoptotic genes. CSE deficient mice cannot sulfhydrate p65, resulting in decreased NF-κB target gene activity and hypersensitivity to TNF-α induced cell death. Thus, sulfhydration of NF-κB appears to be a post-translational modification of p65, which is required for its transcriptional influences on anti-apoptotic genes.

Results

TNF-α induces formation of H_2S by augmenting binding of SP1 to CSE promoter; relationship to CSE influences on cell death

To characterize the influence of CSE on TNF-α mediated cell death, we examined apoptosis in wild type and CSE deleted tissues. Cell death, monitored by TUNEL assay (Figure 1A) and caspase 3 activity (Figure 1B), is markedly augmented in livers of CSE deleted mice treated with TNF-α. In peritoneal macrophages DNA fragmentation (Figure S1A) and caspase 3 activity (Figure S1B) elicited by TNF-α are also substantially increased in CSE knockouts. Treatment of CSE deleted macrophages with the H_2S donor, GYY-4137 (Li et al., 2009; Li et al., 2008) prevents TNF-α induced cell death (Figure 1C).

We examined TNF-α effects upon H_2S formation and observed a tripling, which is prevented in CSE deleted mice (Figure 1D). In peritoneal macrophages treated with TNF-α we also observe a marked time-dependent increase in H_2S formation, which is greatly reduced in preparations from CSE knockouts (Figure 1E).

We explored whether augmented H_2S levels reflect alterations in its biosynthetic enzyme. In mice treated with TNF-α, CSE protein levels are increased 4 – 5 fold (Figure 1F) The stimulation of CSE protein levels in peritoneal macrophages is rapid with increases evident 60 min following TNF-α treatment and maximal at 90-120 min (Figure 1G). To ascertain whether transcriptional activation of CSE is involved, we monitored CSE mRNA levels by RT-PCR (Figure 1H). In peritoneal macrophages TNF-α elicits a pronounced time-dependent increase in CSE mRNA which is maximal at 90 – 120 min. Kimura and associates (Ishii et al., 2004) observed a strong SP1 binding site in the promoter region of CSE, though no binding site for p65 was identified. We measured the binding of SP1 to the

promoter of CSE in peritoneal macrophages by ChIP assay. Binding of SP1 to the CSE promoter is stimulated by TNF-α (Figure 1I and Figure S1C). Depletion of SP1 by RNAi markedly reduces TNF-α mediated augmentation of CSE's mRNA level (Figure 1J) and prevents the stimulation by TNF-α of H_2S production in peritoneal macrophages (Figure 1K). By contrast, depletion of p65 or IKK does not affect CSE level (Figure S1D).These findings suggest that increased occupancy by SP1 of the CSE promoter mediates the enhanced H_2S formation.

CSE regulates DNA binding activity of NF-κB

To ascertain whether augmented levels of H_2S participate in the transcriptional activity of NF-κB, we monitored DNA binding of NF-κB in livers of wt and CSE$^{-/-}$ mice. TNF-α administration markedly enhances NF-κB binding to its DNA targets in the liver with the binding reduced by about 75% in CSE knockout liver (Figure 2A and Figure S2A). In peritoneal macrophages, DNA binding of NF-κB, stimulated by TNF-α, is time-dependent with major reductions in CSE knockout mice (Figure 2B). DNA binding of NF-κB, upon stimulation with TNF-α, was further confirmed by cold-competitor assay (Figure S2B) and antibody supershift assay for p65 (Figure S2C).

We examined the influence of CSE deletion on the activation of NF-κB targets after TNF-α treatment. One of NF-κB's most prominent activities is inhibition of apoptosis upon treatment with TNF-α (Van Antwerp et al., 1996). TNF-α stimulated expression of mRNA (Figure 2C) for anti-apoptotic gene targets of NF-κB, such as *TRAF, cIAP2, Bcl-XL, A20* and *XIAP* (Karin and Lin, 2002; Wang et al., 1998), and protein levels of cIAP2 and Bcl-XL (Figure S2D) is substantially decreased in CSE knockout liver. TNF-α induced mRNA (Figure S2E) and protein (Figure S2F) levels of other p65 cytokine targets, such as CXCL2, CCL2, IL6 and IL8, are also markedly diminished in CSE knockout liver lysate. We explored influences of TNF-α upon binding of p65 to the promoters of anti-apoptotic genes by chromatin immunoprecipitation (ChIP) assay (Figure 2D), as p65 is the subunit of NF-κB that is largely responsible for its anti-apoptotic action (Beg et al., 1995). Binding of p65 to promoters of the anti-apoptotic gene targets *TRAF, cIAP-2, Bcl-XL* and *XIAP* is stimulated by TNF-α in a time-dependent fashion with the time course varying for the different target genes. Binding of p65 to all of these promoters is virtually abolished in macrophages from CSE knockouts.

We wondered whether diminished cysteine levels at selected intracellular microenvironments in CSE deleted cells might be responsible for decreased DNA binding of p65 in CSE$^{-/-}$ macrophages. Supplementation with cysteine does not reverse the deficiencies associated with CSE deletion (Figure S2G). However, overexpressing catalytically active CSE in CSE$^{-/-}$ macrophages rescues these deficiencies, whereas overexpression of a non–PLP (pyridoxal 5'-phosphate)–binding, catalytically inactive mutant CSE (CSE CD) is ineffective (Figure 2E). Treatment with the H_2S donor, GYY-4137 rescues DNA binding activities of NF-κB in TNF-α treated CSE$^{-/-}$ macrophages (Figure 2F). This indicates that catalytic activity of CSE mediates the enhanced transcriptional activity of NF-κB.

Hydrogen sulfide generated by CSE sulfhydrates the p65 subunit of NF-κB at cysteine-38

We wondered whether H_2S, formed by CSE, mediates influences of TNF-α on NF-κB by sulfhydrating its subunit proteins. Sulfhydration (SHY) is a physiological process wherein H_2S attaches an additional sulfur to the thiol (–SH) groups of cysteines yielding a hydropersulfide (–SSH) (Li et al., 2011; Mustafa et al., 2009a; Mustafa et al., 2009b).

We monitored sulfhydration of p65 in liver lysates of TNF-α treated mice by the modified biotin switch assay (Mustafa et al., 2009a). In this assay, free thiols are blocked by MMTS

(methyl methanethiosulfonate) and, to avoid interference by nitrosylated species, we omit ascorbate treatment, which cleaves NO groups from cysteine. Biotin-HPDP is then added to bind free sulfhydryl groups permitting their isolation with streptavidin. As expected, TNF-α-elicited sulfhydration of p65 (SHY-p65) in the liver (Figure S3A) and in peritoneal macrophages (Figure S3B) is abolished in CSE knockouts. Sulfhydration of p65 is time-dependent, being evident in peritoneal macrophages 60 min following TNF-α treatment with a marked increase at 90-120 min (Figure S3C). The process is concentration-dependent, with as little as 5 ng/ml of TNF-α producing detectable sulfhydration (Figure S3D). We also observe sulfhydration of p65 in HEK293 cells overexpressing CSE in the presence of L-cysteine (Figure S3E). The importance of CSE's catalytic activity is apparent in experiments with HEK293 cells overexpressing wt CSE or a non–PLP (pyridoxal 5'-phosphate)–binding catalytically inactive mutant CSE (CSE CD). Sulfhydration of p65 is abolished with overexpression of CSE CD (Figure S3F). Depletion of CSE by RNA interference in peritoneal macrophages also abolishes TNF-α associated sulfhydration of p65 (Figure S3G). The p50 subunit of NF-κB is not sulfhydrated in our experimental conditions. Failure of p50 to be sulfhydrated, despite its reactive C59, appears to reflect disulfide formation with C119, whose mutation to alanine leads to C59 sulfhydration (Figure S4A). However, Binding between p65 and p50 (Figure S4B), as well as DNA binding activity of p50 (Figure S4C), are not altered in CSE deficient macrophages compared to wild type macrophages.

In the modified biotin switch assay for sulfhydration, free SH groups are blocked by MMTS. Failure to completely block such groups might give rise to overestimates of sulfhydration. To further substantiate sulfhydration of p65 and to quantify its levels, we developed an alternative sulfhydration assay employing Alexa Fluor 680 conjugated C2 maleimide (Red Maleimide). We used maleimide, because it interacts selectively with sulfhydryl groups of cysteines, labeling both sulfhydrated as well as unsulfhydrated cysteines. An advantage of this method is that nitrosylated or oxidized cysteines do not react with maleimide. The samples are treated with dithiothreitol (DTT), which selectively cleaves disulfide bonds and so will detach the red signal from sulfhydrated but not unsulfhydrated protein, resulting in decreased fluorescence. We employed the red maleimide detection of overall protein sulfhydration in liver lysates of mice treated with TNF-α (Figure S5A). In wt mice we detect a large number of red bands, representing proteins with SH as well as SSH substituents, with a 50% reduction following DTT treatment. No reduction is evident with CSE deficient liver lysates, establishing that the putative sulfhydration reflects H_2S derived from CSE activity.

Levels of sulfhydration of p65 can be calculated as the residual red fluorescence intensity after DTT treatment divided by the total level of p65 (Figure 3A). In liver lysates of untreated wild-type mice, DTT does not affect levels of "red" p65, indicating the absence of sulfhydration. TNF-α treatment abolishes the red signal in the presence of DTT, indicating sulfhydration of the majority of liver p65 (Figure 3B). This depletion of the red signal reflects the generation of H_2S by CSE, as there is no depletion in the livers of CSE deleted mice. Conceivably DTT might affect the integrity of the p65 antibodies. Accordingly, in some experiments, we washed out the DTT prior to adding the antibodies and have obtained essentially the same results (Figure S4D). Consistent with our findings, DTT treatment under our conditions does not affect the physical integrity and function of IgG antibodies (Okuno and Kondelis, 1978). Treatment with the H_2S donor GYY4137 restores sulfhydration in TNF-α treated HEK 293 cells overexpressing an inactive CSE enzyme (CSE CD) , monitored by the modified biotin switch technique (Figure S4E). The H_2S donor, GYY-4137 rescues sulfhydration of p65 in CSE$^{-/-}$ macrophages (Figure S4F).

In experiments with the Red Maleimide technique, as with the modified biotin switch technique, the effects of TNF-α are time and concentration dependent. Substantial sulfhydration is evident at 60 min and increases to maximal levels at 2 h, when about 75%

of total p65 is sulfhydrated (Figure 3C). As little as 5 ng/ml TNF-α elicits p65 sulfhydration with increasing levels of sulfhydration at 10 and 20 ng/ml (Figure 3D).

To ensure that alterations in H_2S dynamics are not restricted to TNF-α, we examined the effect of lipopolysaccharide (LPS). Increases in CSE protein levels (Figure S4G) and sulfhydration of p65 (Figure S4H) are also evident in peritoneal macrophages isolated from wild type mice 6 h after administration of LPS.

We employed mass spectrometric analysis to identify the cysteine residue responsible for sulfhydration of p65 in mouse liver following treatment of the animals with TNF-α (Figure 3E and S5B). Alexa Fluor 350 conjugated C2 maleimide was added to TNF-α treated and untreated samples. Addition of maleimide to modified p65 elicits a mass increase of 610.21 Da (sulfur= 31.97 + alexa conjugated maleimide = 578.24) compared to untreated proteins in which the increase is 578.24 Da, which is indicated in MS spectrum (Figure S5B). Mass spectrometry reveals a single site of sulfhydration at C38. The maleimide assay confirms that sulfhydration occurs exclusively at C38, as it is abolished in p65-C38S mutants (Figure 3F). It is notable that, though p65 contains 8 cysteines, red staining is abolished with mutation of a single cysteine, C38, whose sulfhydrated state renders it more accessible to reagents than non-sulfhydrated cysteines. This implies that the other 7 cysteines do not have access to maleimide under our experimental conditions. We employed 0.3% Triton X-100 which may not suffice to expose cysteines that are not sulfhydrated. The red maleimide signal increases with greater concentrations of Triton X-100 or Tween 20 (Figure S5C), indicating that more cysteines have interacted with the maleimide. This is consistent with reports that binding between protein and maleimide depends on detergent concentration (Riederer et al., 2008). In our sulfhydration assay, the failure of C38 mutation to reduce the maleimide signal under our conditions (1.2 % Triton X-100) presumably reflects its dilution by signal from the other 7 cysteines (Figure S5D). This conclusion is further supported by mass spectrometric analysis wherein 7 cysteines are able to bind with maleimide (Figure S5E). Thus, with 0.3% Triton X-100, we detect sulfhydration of C38, while with 1.2% Triton X-100, we also observe maleimide modification of the other 7 cysteines along with sulfhydration of C38.

S-nitrosylation of p65 is followed by sulfhydration

Proteins are typically sulfhydrated at reactive cysteines, which are also the sites of physiologic S-nitrosylation (Hess et al., 2005; Jaffrey et al., 2001). Stamler and associates (Kelleher et al., 2007) reported S-nitrosylation of p65 at cysteine-38. We explored the relationship of sulfhydration and nitrosylation, as both processes involve C38. Pronounced sulfhydration is evident at 1-2 h following TNF-α treatment when CSE is induced, whereas iNOS induction is not observed until 5 h after treatment and increases at 8 h (Figure 4A).

To discriminate between sulfhydration and nitrosylation in the same samples, we developed a procedure utilizing a combination of Red and Green Maleimide (Alexa Fluor 488 conjugated C5 maleimide). In this procedure, after treatment with TNF-α, Red Maleimide is added to label sulfhydrated cysteines as well as unmodified cysteines, followed by treatment with ascorbate to remove NO from nitrosylated samples, exposing sulfhydryl groups that can be labeled with Green Maleimide (Figure 4B). As the Green Maleimide specifically labels the nitrosylated species, green fluorescence in TNF-α treated samples directly correlates with nitrosylation.

In primary macrophage cultures at 2 h following TNF-α treatment we detect prominent sulfhydration of p65 but no nitrosylation (Figure 4C). At 5 and 8 h both nitrosylation and sulfhydration are evident. About 80% of total p65 is sulfhydrated at 2 h, decreasing to about 48% and about 18% at 5 h and 8 h respectively, while nitrosylation levels are about 25% at 5

h, increasing to 70% at 8 h (Figure 4D). These levels of sulfhydration and nitrosylation are higher than those reported under basal conditions, (Kelleher et al., 2007; Mustafa et al., 2009a), which presumably reflects the pronounced stimulatory actions of TNF-α upon macrophages. To optimally quantify the extent of sulfhydration and nitrosylation, we treated some samples with maximally effective concentrations of GYY-4137 and GSNO respectively, calculating the effect of TNF-α compared to actions of the H_2S and NO donors. The delayed appearance of nitrosylation in wild type and CSE$^{-/-}$ macrophages (Figure 4E) corresponds to the time-course of iNOS activation (Figure 4A).

As sulfhydration and nitrosylation of p65 respectively stimulate and inhibit (Kelleher et al., 2007) its transcriptional activity, we measured DNA binding affinity of p65 by ChIP assay (Figure S6A). TNF-α enhances binding of p65 to promoters of the anti-apoptotic gene targets *cIAP-2* and *Bcl-XL* at 2 h with a decrease at 5 and 8 h, corresponding to the respective time courses of sulfhydration and nitrosylation. mRNA level of anti-apoptotic genes are augmented at 1-2 h and greatly reduced at 5 h and 8 h following TNF-α treatment. Addition of GYY-4137 to TNF-α treated CSE$^{-/-}$ macrophages rescues the induction of mRNA level of anti-apoptotic genes (Figure S6B). To ascertain whether sulfhydrated p65 can be nitrosylated, we treated p65 with GSNO with or without prior application of GYY4137 (Figure S6C). We observe robust nitrosylation of sulfhydrated p65 (SSNO-p65), almost as great as for the non-sulfhydrated p65, *in vitro*.

If sulfhydration at C38 is critical for transcriptional activity of p65, then activation of NF-κB target genes should be influenced by its mutation. In peritoneal macrophages, TNF-α mediated activation of anti-apoptotic proteins (Figure S6D) and protein level of cytokines (Figure S6E) are markedly reduced in preparations overexpressing p65-C38S, although nuclear translocation of p65-C38S remains unaltered compared to wt p65 (Figure S6F) . Overexpression of CSE in HEK293 cells augments promoter activity of these genes, especially in the presence of added L-cysteine, with stimulation reduced substantially for catalytically inactive CSE (CSE CD) or p65-C38S (Figure 3G).

Sulfhydration of p65 mediates its binding to ribosomal protein S3 (RPS3) to stimulate transcriptional activity

How does sulfhydration of p65 at C38 augment its transcriptional activity? Lenardo and associates (Wan et al., 2007) discovered that ribosomal protein S3 (RPS3) binds to the N-terminal portion of p65 and, as a co-activator, mediates p65 transcriptional activity in the nucleus. To ascertain whether RPS3 plays a role in actions of H_2S on p65, we monitored p65-RPS3 binding in liver lysates (Figure 5A). Under basal conditions the two proteins do not bind, whereas TNF-α treatment of the mice elicits robust binding, which is abolished in CSE $^{-/-}$ animals. The H_2S donor GYY-4137 rescues binding between p65 and RPS3 in TNF-α CSE$^{-/-}$ macrophages (Figure S7A). Conversely, overexpression of wild-type CSE in TNF-α treated HEK293 cells augments binding, but catalytically inactive CSE does not (Figure S7B). To determine the importance of p65-C38 for RPS3 binding, we overexpressed p65-C38S and wt type p65 in RAW 264.7 cells. P65-C38S fails to bind RPS3 upon treatment with TNF-α (Figure 5B).

Because C38 is the common target residue for both H_2S and NO, we explored their relationship in regulating p65-RPS3 interactions. Sulfhydration of p65 peaks at 2 h following TNF-α treatment and declines at 5 and 8 h when it is replaced by nitrosylation (Figure 4A,C). Binding of p65 to RPS3 displays a time course similar to that of p65 sulfhydration with maximal levels at 2 h and a decline at 5 and 8 h in peritoneal macrophages isolated from wt type mice (Figure 5C). In CSE$^{-/-}$ macrophages no binding was observed (data not shown). This suggests that the replacement of sulfhydration at p65-C38 by nitrosylation diminishes p65-RPS3 binding. We directly examined this possibility by

monitoring influences of the H_2S donor GYY-4137 and the NO donor GSNO upon p65-RPS3 binding in TNF-α treated HEK293 cells (Figure 5D). Treatment with GYY-4137 augments p65-RPS3 binding while GSNO abolishes binding. C38S-p65 binds much less than wt p65 to RPS3 upon treatment with GYY-4137, confirming the importance of C38 sulfhydration for p65's binding to RPS3 (Figure S7C).

To assess the role of p65 sulfhydration in RPS3-mediated transcriptional activity, we conducted a ChIP assay for Bcl-XL, a promoter target of p65, utilizing immunoprecipitation with an antibody to RPS3 (Figure 5E). TNF-α treatment of RAW 264.7 cells elicits binding of RPS3 to the p65-Bcl-XL promoter with peak binding evident at 2 h and a marked diminution at 5 and 8 h, corresponding to the time course for sulfhydration of p65 (Figure 5E). To substantiate the notion that H_2S augments promoter interactions while NO blocks them, we treated HEK293 cells with GYY-4137 and GSNO along with TNF-α (Figure S7D). GYY-4137 activates the binding of RPS3 to p65-Bcl-XL promoter, while GSNO does not. Promoter occupancy is mediated by sulfhydration of p65 at C38, because stimulation of both Bcl-XL and cIAP promoters is abolished with P65-C38S mutation of p65 (Figure 5F). Binding of p65 to the promoter of the anti-apoptotic genes *cIAP2, TRAF, A20* and *Bcl-XL* requires RPS3, as its depletion by RNA interference prevents activation of Bcl-XL (Figure 5G). This suggests that binding of sulfhydrated p65 to RPS3 is important for DNA binding activity of NF-κB. In CSE deficient cells, DTT does not affect the binding of p65 to RPS3, presumably because p65 cannot be sulfhydrated (Figure S7E). In cell lysates at 2 h following TNF-α treatment, when sulfhydration of p65 predominates (Figure S8A), DTT decreases p65-RPS3 binding, presumably by decreasing p65 sulfhydration (Figure S8C). By contrast, at 5 and 8 h, when p65-nitrosylation is dominant, DTT enhances the binding, evidently by removing the NO group and freeing up the cysteine sulfhydryl that mediates RPS3 binding. CHIP analysis of Bcl-XL promoter binding by p65 reveals similar effects of DTT (Figure S8E). At 2 h following TNF-α treatment, GSH exerts negligible effects on p65 sulfhydration (Figure S8B), RPS3 binding (Figure S8D) and DNA binding (Figure S8F), presumably reflecting negligible effects of sulfhydration. At 5 and 8 h following TNF-α treatment, effects of GSH on these parameters resemble those of DTT but are substantially less, reflecting weaker effects than DTT upon nitrosylation (Paige et al., 2008). Direct modification of RPS3 itself by the gasotransmitters does not participate in gene activation, as we have been unable to detect any sulfhydration or nitrosylation of RPS3 protein (data not shown).

We wondered whether association between sulfhydrated p65 and RPS3 impacts cell death. In RAW 264.7 cells, DNA fragmentation elicited by TNFα is substantially increased in cells overexpressing p65-C38S compared to wt p65 (Figure 5H), indicating that C38 sulfhydration of p65 is important for its anti-apoptotic function. To ascertain whether these actions of p65 require its binding to RPS3, we depleted RPS3 by RNA interference. DNA fragmentation is markedly increased in RPS3 depleted cells. Overexpression of wt p65 or P65-C38S fails to rescue TNF-α mediated cell death in RPS3 depleted cells, confirming the importance of p65's binding to RPS3 for activation of anti-apoptotic genes.

Discussion

In the present study we have identified a signaling cascade that mediates the anti-apoptotic actions of NFκB in response to TNFα activation (Figure S9I). TNF-α stimulates transcription of the H_2S generating enzyme CSE, whose promoter region has a recognition motif for SP1, a transcription factor activated by TNFα. The synthesized H_2S sulfhydrates the p65 subunit of NF-κB at cysteine-38 which augments its ability to bind its co-activator RPS3. The activator/co-activator complex then stimulates transcription of anti-apoptotic genes.

We have measured sulfhydration of p65 both by the modified biotin switch assay and the maleimide assay. Maleimides do not react with methionine, histidine or tyrosine, instead specifically targeting thiol groups of cysteine residues. In proteins with multiple cysteine residues, the reactivity of an individual cysteine is dependent both on its local environment and the hydrophobicity of the reactive dye (Brustad et al., 2008; Kim et al., 2008; Tyagarajan et al., 2003). Moreover, the polarity of Alexa Fluor conjugated maleimides permits the sensitive detection of exposed or accessible thiols (Gelderman et al., 2006; Sahaf et al., 2003). This may explain the fact that in our assay system Alexa conjugated C2 or C5 maleimide interacts selectively with cysteine-38 of p65. The similarity of results with the maleimide and modified biotin switch methods supports the reliability of the two techniques as assays for sulfhydration. The exact molecular mechanism, whereby the modified biotin switch assay differentiates sulfhydrated and unmodified cysteine is not altogether clear. We presume that MMTS can react with both but that biotin selectively links to the more chemically reactive sulfhydryl moiety.

Lenardo and associates (Wan et al., 2007) established that RPS3 mediates interactions of p65 with its gene promoter targets. Heretofore, specific cellular functions of RPS3 have not been delineated. Our findings establish an important role for RPS3 in mediating the anti-apoptotic influences of p65. Sulfhydration of p65 enables it to bind to RPS3 whose co-activator effects are required for transcriptional activation. Earlier studies have shown that oxidizing and reducing agents, such as DTT, respectively decrease and increase p65 binding to DNA (Gius et al., 1999). In our study, DTT (up to around 2 mM) treatment of intact cells also enhances p65 binding to DNA due to increases in p65 sulfhydration and binding to RPS3, findings that may account for the earlier observations. Higher concentrations of DTT (2.5 mM and above), abolish sulfhydration of p65, which in turn decreases its binding to RPS3 and its DNA binding to promoters of anti-apoptotic genes leading to cell death. Interestingly, C38 of p65 lies in the DNA binding domain, and its sulfhydration enhances binding to RPS3 leading to increased transcriptional activation by p65. Exactly how p65, RPS3 and the target DNA promoters interface is unclear and presumably awaits structural studies.

Sulfhydration and nitrosylation both appear to regulate p65 and do so reciprocally. Following TNF-α treatment, sulfhydration of p65 occurs first, leading to an early activation of its promoter targets. Subsequently, NO generated by iNOS nitrosylates p65, which reverses the sulfhydration-elicited activation. Conceivably, reciprocal influences of sulfhydration and nitrosylation represent a mode for determining NF-κB physiology and, perhaps, actions of other signaling proteins.

NF-κB mediates inflammatory effects of TNF-α with ramifications for diseases such as arthritis, diabetes, sepsis and osteoporosis (Ghosh and Karin, 2002). NF-κB physiologically suppresses the pro-apoptotic effects of TNF-α, leading to diminished apoptosis. Our findings indicate that the anti-apoptotic actions of NF-κB are dependent on the generation of H_2S which sulfhydrates p65. Decreasing p65 sulfhydration and thereby augmenting apoptosis may be beneficial in the therapy of diseases that involve excessive cell growth and division, such as cancer.

Supplementary Material

Refer to Web version on PubMed Central for supplementary material.

Acknowledgments

Experimental Procedures

Maleimide assay

To monitor linkage of maleimide and p65, cells were homogenized with lysis buffer using various concentrations of Triton X-100 (0-1.5%) or Tween 20 (0-2% v/v) and immunoprecipitated with anti-p65 antibody. After washing beads with the same buffer, they were incubated with Alexa Fluor 680 conjugated C2 maleimide (Red Maleimide) (2 μM, final concentration) and kept for 2 h at 4°C with occasional gentle mixing. Beads were pelleted, washed and suspended in 2X SDS-PAGE buffer for gel electrophoresis. Gels were transferred to PVDF membranes, which were scanned with the Li-COR Odyssey system. The intensity of red fluorescence of p65 was quantified using software attached to the Odyssey system. These membranes were also employed for western blotting with anti-p65 antibody.

This assay was designed based on the principles described before (Aracena-Parks et al., 2006; Wright et al., 2006). Liver tissues or cells treated with or without TNF-α were homogenized in lysis buffer (150 mM NaCl, 0.5% v/v Tween 20, 50 mM Tris 7.5 and 1 mM EDTA) and immunoprecipitated with anti-p65 antibody. After washing beads with the same buffer, beads were incubated with Alexa Fluor 680 conjugated C2 maleimide (Red Maleimide) (2 μM, final concentration) and kept for 2 h at 4°C with occasional gentle mixing. The beads were pelleted and washed with the same buffer, then treated with or without DTT (1 mM, final concentration) for 1 h at 4°C. Beads were pelleted, washed and suspended in 2X SDS-PAGE buffer for gel electrophoresis. Gels were transferred to PVDF membranes, which were scanned with the Li-COR Odyssey system. The intensity of red fluorescence of p65 was quantified using software attached to the Odyssey system. These membranes were also employed for western blotting with anti-p65 antibody.

To distinguish between nitrosylation and sulfhydration of p65, liver tissues or cells with or without TNF-α exposure were homogenized in lysis buffer (150 mM NaCl, 0.5% v/v Tween 20, 50 mM Tris 7.5 and 1 mM EDTA) and immunoprecipitated with anti-p65 antibody. After washing beads with the same buffer, beads were incubated with Alexa Fluor 680 conjugated C2 maleimide (Red Maleimide) (2 μM, final concentration) and kept for 2 h at 4°C with occasional gentle mixing. The beads were pelleted and washed with the same buffer. At this point, ascorbic acid was added and preparations kept at 4°C for 1 h with occasional mixing. Beads were pelleted and mixed either with Alexa Fluor 488 conjugated C5 maleimide or IRDye® 800CW (Green Maleimide) (2 μM) and maintained for 2 h at 4°C with occasional gentle mixing. The beads were pelleted and washed with same buffer. The beads were treated with or without DTT (1 mM) for 1 h at 4°C, pelleted, washed and suspended in 2X SDS-PAGE buffer followed by electrophoresis. Gels were scanned with the Li-COR Odyssey system. The intensity of red and green fluorescence of p65 was quantified using software attached to the Odyssey system.

To measure nitrosylation of sulfhydrated p65 protein, it was treated with GYY-4137(200 μM) for 30 min and passed through a desalting column to remove excess GYY-4137. Part of this sample was treated with GSNO (200 μM) for 30 min and again passed through a desalting column to remove excess GSNO. Modified proteins were treated with ascorbate followed by Alexa Fluor 488 conjugated C5 maleimide (Green Maleimide) (2 μM) and maintained for 1 h at 4°C with occasional gentle mixing. Then samples were treated with DTT (1 mM) for 1 h at 4°C and suspended in 2X SDS-PAGE buffer followed by electrophoresis. Gels were scanned with the Li-COR Odyssey system.

To determine whether DTT influences the p65 antibody used for immunoprecipitation assays, we incubated p65 antibody with or without 1 mM of DTT for 45 min prior to immoprecipation experiments with RAW264.7 cell lysates. Secondary antibody conjugated beads were added, pelleted, washed and suspended in 2X SDS-PAGE buffer followed by electrophoresis. The intensity of protein bands was measured by Image J software.

Mass spectrometric analysis

Wild type mice were treated with TNF-α (10 μg/kg) for 4 h, sacrificed, perfused and livers were isolated. Livers were lysed in RIPA-A (0.3% or 1.2 % Triton X-100, 50 mM Tris pH 7.4 and 1 mM EDTA) with rotation at 4 °C for 30 min. Liver lysates were centrifuged at 14,000 g for 10 min followed by p65 immunoprecipitation with anti-p65 antibody. After washing with the same buffer, beads were incubated with Alexa Fluor 350 conjugated C5 maleimide (2 μM, final concentration) and kept for 2 h at 4°C with occasional gentle mixing. The beads were pelleted and washed with same buffer. Beads were suspended in $2 \times$ SDS-PAGE buffer and visualized by colloidal Coomassie staining. Gel-purified p65 was chymotryptic-digested and analyzed by LC-MS/MS.

CSE activity assays

CSE activity was assessed by measuring H_2S production as described previously (Mustafa et al., 2009a). Briefly, the assay was carried out in a 250 μl reaction mixture containing 10 mM potassium phosphate buffer saline (pH 7.4), 10 mM L-cysteine, 15 μM PLP, and 10% (w/v) homogenate. High-performance liquid chromatography (HPLC) injection vials (2 ml) containing the reaction mixtures were flushed with N_2 before being sealed. Reactions were initiated by transferring the vials from ice to a 37°C shaking water bath. After incubating at 37°C for 60 min, the reaction was terminated by injecting a mixture of 125 μl of 1% zinc acetate and 2.5 μl of 10 N NaOH trapping solution. The vials were horizontally shaken for another 60 min to ensure complete trapping of H_2S released from the mixture. Then, 0.5 ml of water was added to each vial followed by 0.1 ml of 20 mM N,N-dimethyl-p-phenylenediamine sulfate in 7.2 M HCl, immediately followed by addition of 0.1 ml of 30 mM $FeCl_3 \cdot 6H2O$ in 1.2 M HCl. Absorbance of the resulting solution at 670 nm was measured 20 min later with a spectrophotometer. H_2S content was calculated using a calibration curve of standard H_2S solutions prepared with NaHS.

Modified biotin switch (sulfhydration) assay

The assay was carried out as described previously (Mustafa et al., 2009a) with modifications. Briefly, liver tissues or cells treated with or without TNF-α were homogenized in HEN buffer [250 mM Hepes-NaOH (pH 7.7), 1 mM EDTA, and 0.1 mM neocuproine] supplemented with 100 μM deferoxamine and centrifuged at $13,000 \times g$ for 30 min at 4°C. Cell lysates (240 μg) were added to blocking buffer (HEN buffer adjusted to 2.5% SDS and 20 mM MMTS) at 50°C for 20 min with frequent vortexing. The MMTS was then removed by acetone and proteins precipitated at –20°C for 20 min. After acetone removal, the proteins were resuspended in HENS buffer (HEN buffer adjusted to 1% SDS). To the suspension 4 mM biotin-HPDP was added without ascorbic acid. After incubation for 3 h at 25°C, biotinylated proteins were precipitated by streptavidin-agarose beads, which were then washed with HENS buffer. The biotinylated proteins were eluted by SDS–polyacrylamide gel electrophoresis (SDS-PAGE) sample buffer and subjected to western blot analysis. For quantitation of protein sulfhydration, samples were run on blots alongside total lysates ("loads") and subjected to immunoblotting with antibodies specific to each protein.

Gene expression analysis

For real-time PCR, total RNA was isolated using RNeasy kits (Qiagen) primed with random hexamer oligonucleotides and reverse transcribed using an Invitrogen First Strand cDNA synthesis kit. PCR was performed using a SYBR Green master mix, and all data were normalized to 18s rRNA. For protein microarray, liver lysates or culture supernatants were tested using the Raybiotech cytokine antibody microarray (Raybiotech, Norcross, GA) as described previously (Chaisson et al., 2002). The strengths of the signals were determined by densitometry.

Chromatin immunoprecipitation (ChIP)

Chromatin immunoprecipitation was performed using the ChIP assay kit from Upstate Biotech according to the manufacturer's instructions. Antibodies used included anti-p65 (C-20) (Santa Cruz Biotech) anti-RPS3 (Cell Signaling) and anti-SP1(Santa Cruz Biotech). Anti- rabbit IgG fron Santa Cruz Biotechnology (Santa Cruz, CA) was used as a control. We have used -391 to -221 bp region of CSE promoter as a control of irrelevant region of DNA.

Electrophoretic mobility shift assay (EMSA) and luciferase assay

NF-κB consensus double stranded oligonucleotides (5'-AGTTGAGGGGACTTTCCCAGG-3') were purchased from Santa Cruz Biotechnology. They were first end-labeled with $[\gamma^{32P}]$ATP (Amersham Biosciences, Piscataway, New Jersey) using the T4 polynucleotide kinase (Promega, Madison, Wisconsin). Binding reactions were prepared using 1 to 5 μg of total cellular extract or liver extracts with 50,000 cpm of oligonucleotides in a 25 μl reaction volume containing 10 mM HEPES/KOH pH 7.9), 50 mM KCl, 2.5 mM MgCl2, 10% glycerol, 1 μg DNAse free bovine serum albumin and 2.5 μg poly[d(I-C)] at room temperature for 30 min. Binding reactions were resolved on a 4% non-denaturing polyacrylamide gel at 22 mA for 3 h at 4°C in 1x TBE. Gels were subsequently dried, exposed to a phosphor screen and visualized on a phosphoimager (Amersham Biosciences). Densitometry was conducted with ImageQuant 5.2 software (Amersham Biosciences). For competition assays, a 1, 5, 10 and 15 fold molar excess of unlabelled probe was added as a competitor 30 min before the addition of the labelled probe. For characterisation of κB binding proteins, the reactions were supplemented with affinity purified rabbit polyclonal antibodies against mouse p65 antibody (Santa Cruz Biotechnology, Santa Cruz, CA), 30 min before electrophoresis, as described previously (Lenardo and Baltimore, 1989).

For luciferase reporter assays, firefly luciferase constructs driven by NF-kB binding sequences and Renilla luciferase pRL-TK (Int-) plasmid were used (Promega). Lysates were analyzed using the Dual-Luciferase Kit (Promega), with firefly fluorescence units normalized to Renilla luciferase fluorescence units.

RT–PCR analysis

Total RNA was extracted from liver tissue or cells using Trizol reagent (Invitrogen) according to the manufacturer's instructions. Reverse transcription as well as PCR procedures used Superscript One Step RT–PCR with Platinum Taq (Invitrogen).

References

Aracena-Parks P, Goonasekera SA, Gilman CP, Dirksen RT, Hidalgo C, Hamilton SL. Identification of cysteines involved in S-nitrosylation, S-glutathionylation, and oxidation to disulfides in ryanodine receptor type 1. J Biol Chem. 2006; 281:40354–40368. [PubMed: 17071618]

Beg AA, Baltimore D. An essential role for NF-kappaB in preventing TNF-alpha-induced cell death. Science. 1996; 274:782–784. [PubMed: 8864118]

Beg AA, Sha WC, Bronson RT, Ghosh S, Baltimore D. Embryonic lethality and liver degeneration in mice lacking the RelA component of NF-kappa B. Nature. 1995; 376:167–170. [PubMed: 7603567]

Brustad EM, Lemke EA, Schultz PG, Deniz AA. A general and efficient method for the site-specific dual-labeling of proteins for single molecule fluorescence resonance energy transfer. J Am Chem Soc. 2008; 130:17664–17665. [PubMed: 19108697]

Chaisson ML, Brooling JT, Ladiges W, Tsai S, Fausto N. Hepatocyte-specific inhibition of NF-kappaB leads to apoptosis after TNF treatment, but not after partial hepatectomy. J Clin Invest. 2002; 110:193–202. [PubMed: 12122111]

Delhase M, Hayakawa M, Chen Y, Karin M. Positive and negative regulation of IkappaB kinase activity through IKKbeta subunit phosphorylation. Science. 1999; 284:309–313. [PubMed: 10195894]

Gelderman KA, Hultqvist M, Holmberg J, Olofsson P, Holmdahl R. T cell surface redox levels determine T cell reactivity and arthritis susceptibility. Proc Natl Acad Sci U S A. 2006; 103:12831–12836. [PubMed: 16908843]

Ghosh S, Karin M. Missing pieces in the NF-kappaB puzzle. Cell. 2002; 109(Suppl):S81–96. [PubMed: 11983155]

Gius D, Botero A, Shah S, Curry HA. Intracellular oxidation/reduction status in the regulation of transcription factors NF-kappaB and AP-1. Toxicol Lett. 1999; 106:93–106. [PubMed: 10403653]

Hess DT, Matsumoto A, Kim SO, Marshall HE, Stamler JS. Protein S-nitrosylation: purview and parameters. Nat Rev Mol Cell Biol. 2005; 6:150–166. [PubMed: 15688001]

Ishii I, Akahoshi N, Yu XN, Kobayashi Y, Namekata K, Komaki G, Kimura H. Murine cystathionine gamma-lyase: complete cDNA and genomic sequences, promoter activity, tissue distribution and developmental expression. Biochem J. 2004; 381:113–123. [PubMed: 15038791]

Jaffrey SR, Erdjument-Bromage H, Ferris CD, Tempst P, Snyder SH. Protein S-nitrosylation: a physiological signal for neuronal nitric oxide. Nat Cell Biol. 2001; 3:193–197. [PubMed: 11175752]

Karin M, Ben-Neriah Y. Phosphorylation meets ubiquitination: the control of NF-[kappa]B activity. Annu Rev Immunol. 2000; 18:621–663. [PubMed: 10837071]

Karin M, Lin A. NF-kappaB at the crossroads of life and death. Nat Immunol. 2002; 3:221–227. [PubMed: 11875461]

Kelleher ZT, Matsumoto A, Stamler JS, Marshall HE. NOS2 regulation of NF-kappaB by S-nitrosylation of p65. J Biol Chem. 2007; 282:30667–30672. [PubMed: 17720813]

Kim Y, Ho SO, Gassman NR, Korlann Y, Landorf EV, Collart FR, Weiss S. Efficient site-specific labeling of proteins via cysteines. Bioconjug Chem. 2008; 19:786–791. [PubMed: 18275130]

Kimura H. Hydrogen sulfide: from brain to gut. Antioxid Redox Signal. 2010; 12:1111–1123. [PubMed: 19803743]

Lenardo MJ, Baltimore D. NF-kappa B: a pleiotropic mediator of inducible and tissue-specific gene control. Cell. 1989; 58:227–229. [PubMed: 2665943]

Li L, Rose P, Moore PK. Hydrogen sulfide and cell signaling. Annu Rev Pharmacol Toxicol. 2011; 51:169–187. [PubMed: 21210746]

Li L, Salto-Tellez M, Tan CH, Whiteman M, Moore PK. GYY4137, a novel hydrogen sulfide-releasing molecule, protects against endotoxic shock in the rat. Free Radic Biol Med. 2009; 47:103–113. [PubMed: 19375498]

Li L, Whiteman M, Guan YY, Neo KL, Cheng Y, Lee SW, Zhao Y, Baskar R, Tan CH, Moore PK. Characterization of a novel, water-soluble hydrogen sulfide-releasing molecule (GYY4137): new insights into the biology of hydrogen sulfide. Circulation. 2008; 117:2351–2360. [PubMed: 18443240]

Mustafa AK, Gadalla MM, Sen N, Kim S, Mu W, Gazi SK, Barrow RK, Yang G, Wang R, Snyder SH. H2S signals through protein S-sulfhydration. Sci Signal. 2009a; 2:ra72. [PubMed: 19903941]

Mustafa AK, Gadalla MM, Snyder SH. Signaling by gasotransmitters. Sci Signal. 2009b; 2:re2. [PubMed: 19401594]

Okuno T, Kondelis N. Evaluation of dithiothreitol (DTT) for inactivation of IgM antibodies. J Clin Pathol. 1978; 31:1152–1155. [PubMed: 34632]

Paige JS, Xu G, Stancevic B, Jaffrey SR. Nitrosothiol reactivity profiling identifies S-nitrosylated proteins with unexpected stability. Chem Biol. 2008; 15:1307–1316. [PubMed: 19101475]

Riederer IM, Herrero RM, Leuba G, Riederer BM. Serial protein labeling with infrared maleimide dyes to identify cysteine modifications. J Proteomics. 2008; 71:222–230. [PubMed: 18556256]

Sahaf B, Heydari K, Herzenberg LA. Lymphocyte surface thiol levels. Proc Natl Acad Sci U S A. 2003; 100:4001–4005. [PubMed: 12642656]

Szabo C. Hydrogen sulphide and its therapeutic potential. Nat Rev Drug Discov. 2007; 6:917–935. [PubMed: 17948022]

Thuret JY, Valay JG, Faye G, Mann C. Civ1 (CAK in vivo), a novel Cdk-activating kinase. Cell. 1996; 86:565–576. [PubMed: 8752211]

Tyagarajan K, Pretzer E, Wiktorowicz JE. Thiol-reactive dyes for fluorescence labeling of proteomic samples. Electrophoresis. 2003; 24:2348–2358. [PubMed: 12874870]

Van Antwerp DJ, Martin SJ, Kafri T, Green DR, Verma IM. Suppression of TNF-alpha-induced apoptosis by NF-kappaB. Science. 1996; 274:787–789. [PubMed: 8864120]

Wan F, Anderson DE, Barnitz RA, Snow A, Bidere N, Zheng L, Hegde V, Lam LT, Staudt LM, Levens D, et al. Ribosomal protein S3: a KH domain subunit in NF-kappaB complexes that mediates selective gene regulation. Cell. 2007; 131:927–939. [PubMed: 18045535]

Wang CY, Mayo MW, Korneluk RG, Goeddel DV, Baldwin AS Jr. NF-kappaB antiapoptosis: induction of TRAF1 and TRAF2 and c-IAP1 and c-IAP2 to suppress caspase-8 activation. Science. 1998; 281:1680–1683. [PubMed: 9733516]

Wright CM, Christman GD, Snellinger AM, Johnston MV, Mueller EG. Direct evidence for enzyme persulfide and disulfide intermediates during 4-thiouridine biosynthesis. Chem Commun (Camb). 2006:3104–3106. [PubMed: 16855700]

Yang G, Wu L, Jiang B, Yang W, Qi J, Cao K, Meng Q, Mustafa AK, Mu W, Zhang S, et al. H2S as a physiologic vasorelaxant: hypertension in mice with deletion of cystathionine gamma-lyase. Science. 2008; 322:587–590. [PubMed: 18948540]
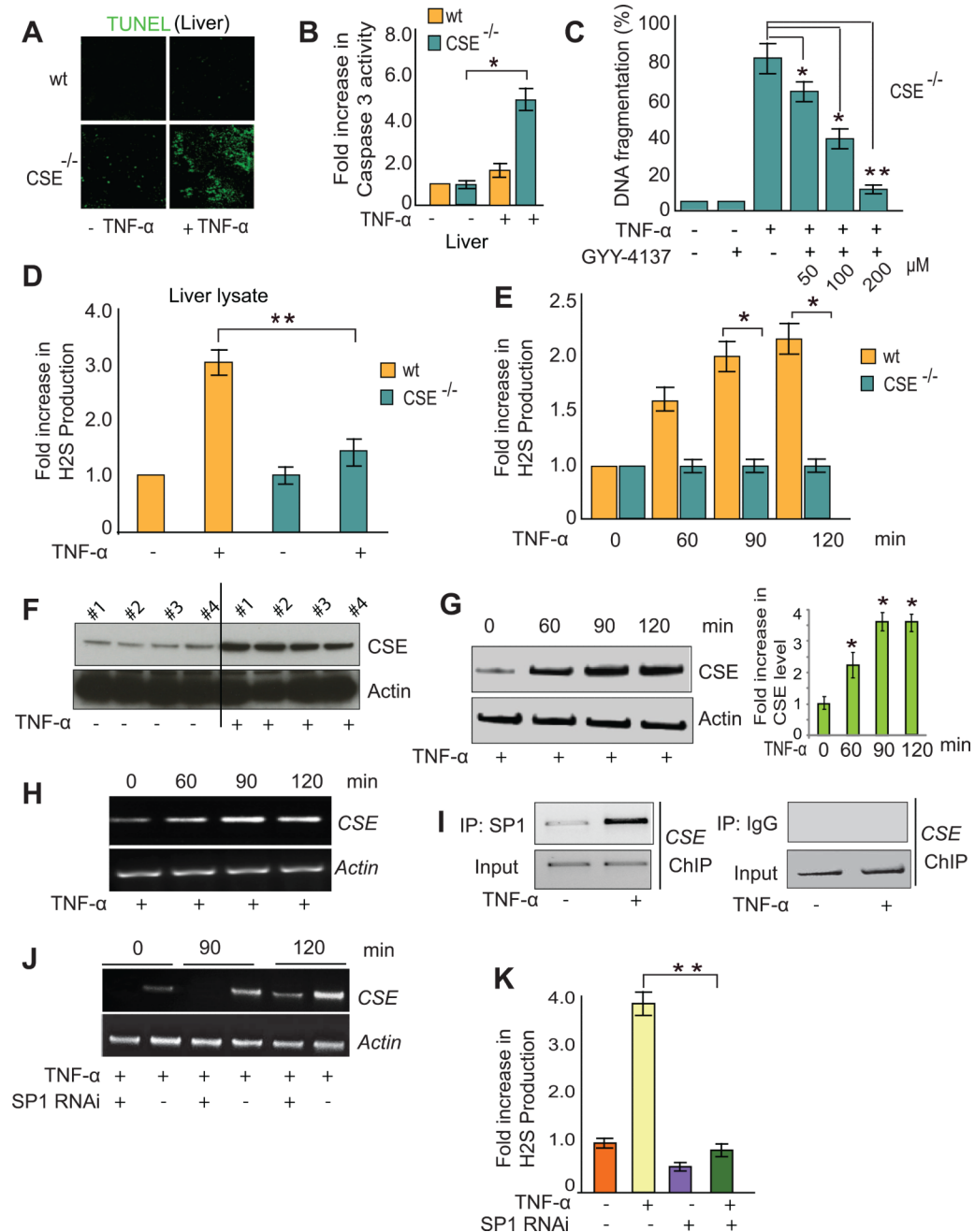
Figure 1. CSE^-/- mice are more susceptible to TNF-α induced cell death; TNF-α stimulates hydrogen sulfide production by stimulating CSE transcription via SP1

(**A**) Treatment withTNF-α elicits more TUNEL positive cells in liver of CSE^-/- than wild type mice. (**B**) Caspase 3 activation is increased in CSE^-/- mice liver following TNF-α treatment. *p < 0.01, n = 5, one-way ANOVA, mean ± SEM. (**C**) DNA fragmentation induced by TNF-α in macrophages isolated from CSE^-/- mice is decreased by pretreatment with GYY-4137 in a concentration dependent manner. *p < 0.01, n = 5, one-way ANOVA, mean ± SEM. **p < 0.001, n = 5, one-way ANOVA, mean ± SEM. (**D**) TNF-α stimulation of hepatic H_2S formation is abolished in CSE^-/- mice. Wild type and CSE^-/- mice were injected with TNF-α and H_2S formation assayed in liver lysates. **p < 0.001, n = 5, one-way ANOVA, mean ± SEM. (**E**) TNF-α stimulation of H_2S formation in peritoneal

macrophages is diminished in CSE$^{-/-}$ preparations. *p < 0.01, n = 3, oneway ANOVA, mean ± SEM. (**F**) TNF-α treatment increases hepatic CSE protein level (n=4). (**G**) TNF-α causes an increase in CSE protein level in peritoneal macrophages in time dependent manner. Densitometric analysis of CSE protein level in TNF-α treated macrophages. *p < 0.01, n = 5, one-way ANOVA, mean ± SEM. (**H**) TNF-α causes an increase in peritoneal macrophage CSE mRNA levels in time dependent manner. (**I**) TNF-α-elicited enhancement of SP1 binding to the CSE promoter. (**J**) SP1 RNAi treatment prevents TNF-α stimulation of CSE mRNA in peritoneal macrophages.(**K**) Treatment with SP1 RNAi reduces TNF-α-elicited H$_2$S formation in peritoneal macrophages. **p < 0.001, n = 5, one-way ANOVA, mean ± SEM.
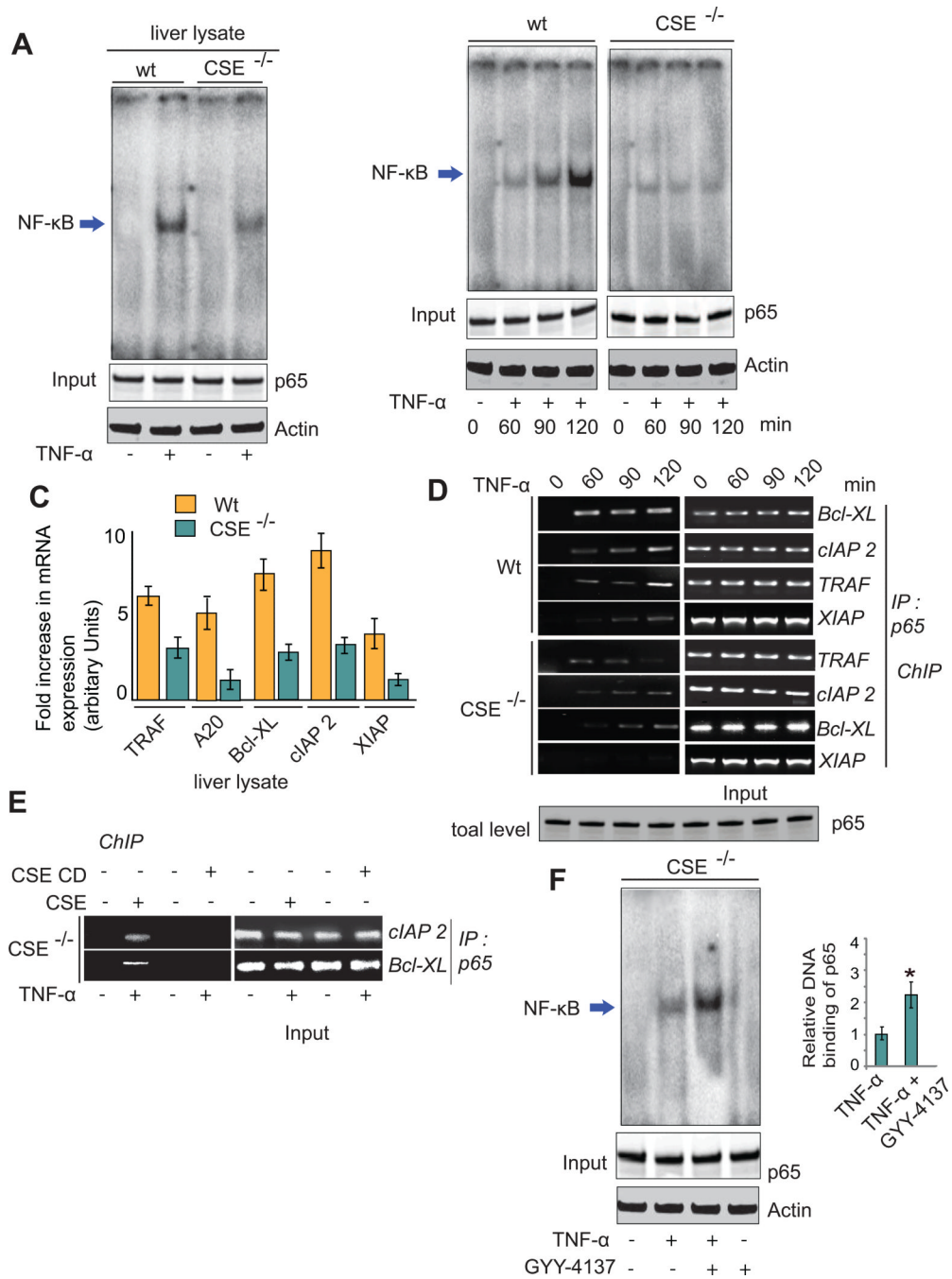
Figure 2. Transcriptional activity of p65 is reduced in CSE⁻/⁻ mice

(**A**) DNA binding of NF-κB is reduced in CSE⁻/⁻ mice. Wild type and CSE⁻/⁻ mice were injected with TNF-α, and liver lysates subjected to EMSA assay. (**B**) In peritoneal macrophages TNF-α stimulates DNA binding of NF-κB in a time dependent manner, effects abolished in CSE⁻/⁻ mice. (**C**) Anti-apoptotic gene expression is reduced in CSE⁻/⁻ mice. Wild type and CSE⁻/⁻ mice were injected with TNF-α, and mRNA levels of anti-apoptotic genes measured by real time RT-PCR. *p < 0.01, n = 5, one-way ANOVA, mean ± SEM. (**D**) Reduced binding of p65 to promoters of anti-apoptotic genes in CSE⁻/⁻ mice treated with TNF-α. (**E**) Overexpression of wild type CSE in CSE⁻/⁻ macrophages can rescue binding of p65 to promoters of anti-apoptotic genes. Overexpressed catalytically dead CSE mutant

(CSE CD) in CSE$^{-/-}$ macrophages fails to rescue binding of p65 to promoters of anti-apoptotic genes. **(F)** DNA binding of NF-κB is rescued in TNF-α treated CSE$^{-/-}$ macrophages after treatment with GYY-4137 (200 μM). *p < 0.01, n = 5, one-way ANOVA, mean ± SEM.
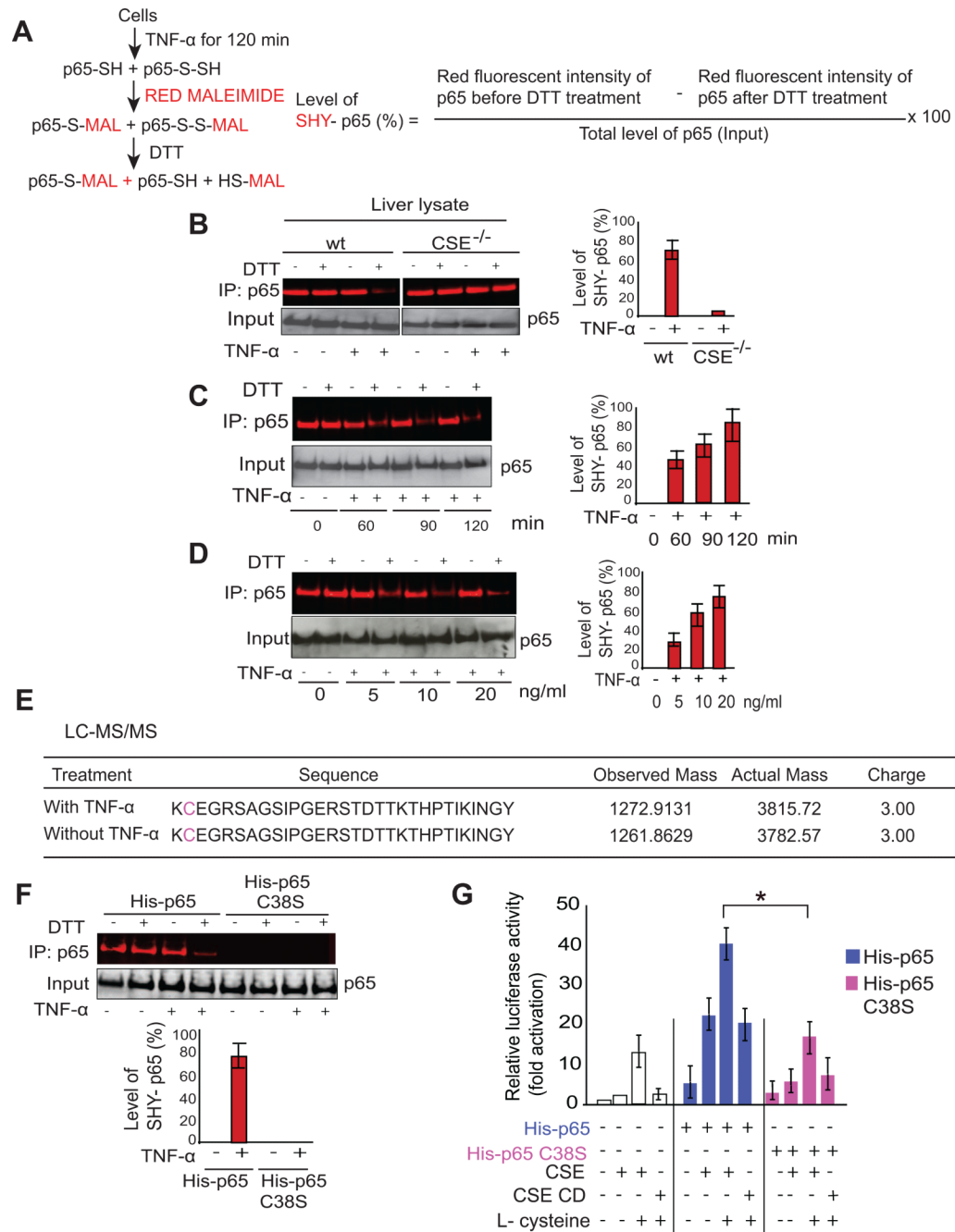
Figure 3. Sulfhydration of p65-C38, detected by maleimide assay, enhances its binding to canonical NF-κB DNA sequences

(**A**) Schematic diagram for detection of p65 sulfhydration using red maleimide. (**B**) Depletion of red fluorescence intensity in TNF-α treated mice after DTT treatment establishes sulfhydration of p65. Data are presented as mean ± SEM. (**C**) Time dependent decrease in red fluorescence intensity of p65 protein in TNF-α treated macrophages associated with sulfhydration of p65. Data are presented as mean ± SEM. (**D**) Concentration dependent decrease in red fluorescence intensity of p65 protein in TNF-α treated macrophages reflecting sulfhydration of p65. Data are presented as mean ± SEM. (**E**) LC-MS/MS analysis of endogenous full-length p65 protein treated with TNF-α (10 μg/kg) for 4

h reveals sulfhydration of Cys38. **(F)** Abolition of red fluorescence intensity in C38S mutant of p65 indicates that C38 is the site for sulfhydration. Data are presented as mean ± SEM. **(G)** Luciferase activity of p65 but not p65-C38S is enhanced by transfection of CSE. *p < 0.01, n = 4, one-way ANOVA, mean ± SEM.
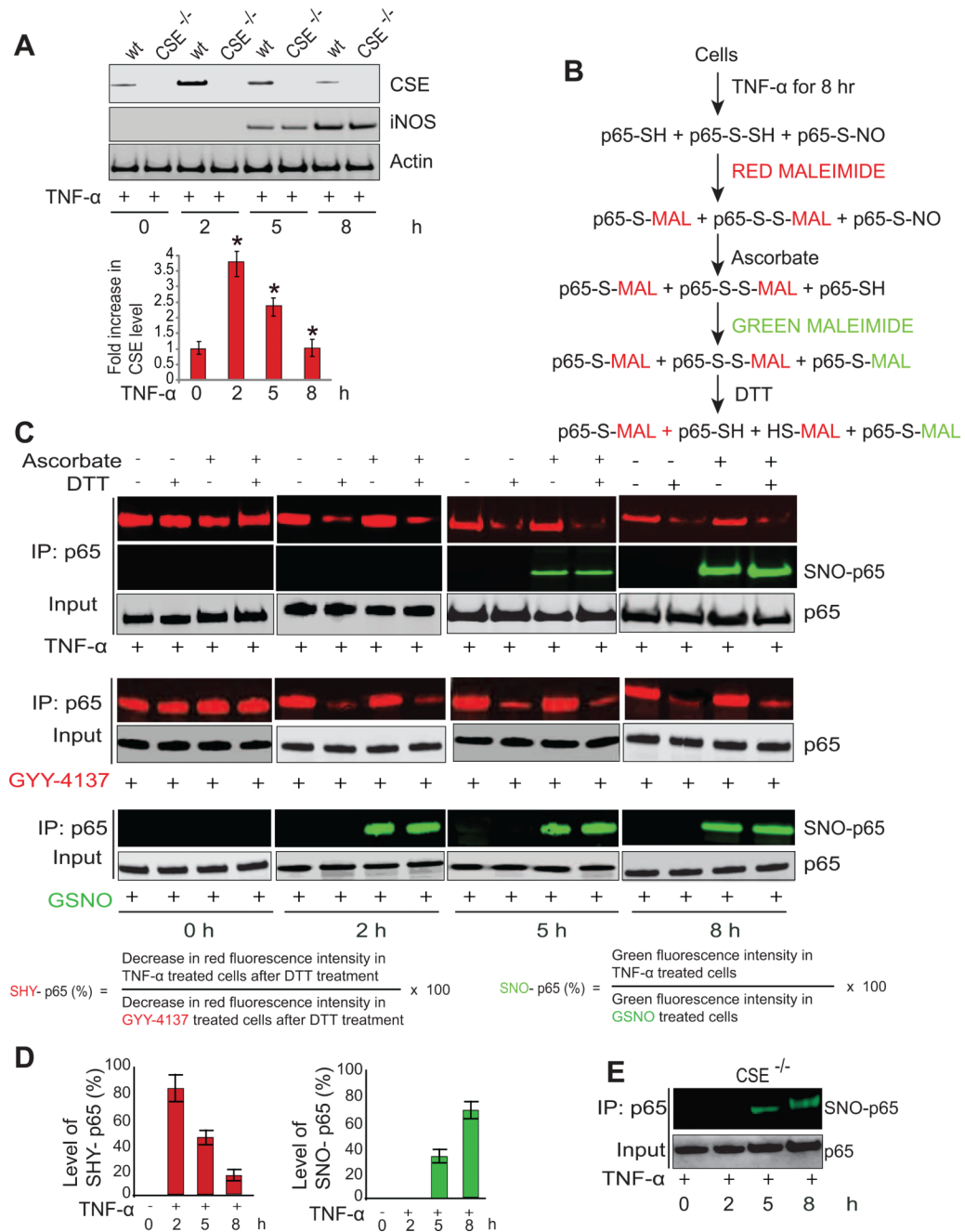
Figure 4. Detection of nitrosylation and sulfhydration of p65 by maleimide assay
(**A**) Levels of CSE and iNOS in TNF-α treated macrophages upon treatment with TNF-α for 8h. Densitometric analysis of CSE protein level in macrophages after treatment with TNF-α for 8 h. *p < 0.001, n = 3, one-way ANOVA, mean ± SEM. (**B**) Schematic diagram for detection of sulfhydration and nitrosylation of p65 using red and green maleimide. (**C**) Time dependent changes in sulfhydration and nitrosylation of p65 in TNF-α treated macrophages. As a positive control, we have measured sulfhydration and nitrosylation of p65 upon treatment with GYY-4137 (800 μM) or GSNO (500 μM) for 0, 2, 5 and 8 h. (**D**) Assessment of sulfhydration and nitrosylation of p65 at various times in TNF-α treated cells. Data are

presented as mean ± SEM. **(E)** Levels of nitrosylation of p65 in TNF-α treated CSE $^{-/-}$ macrophages.
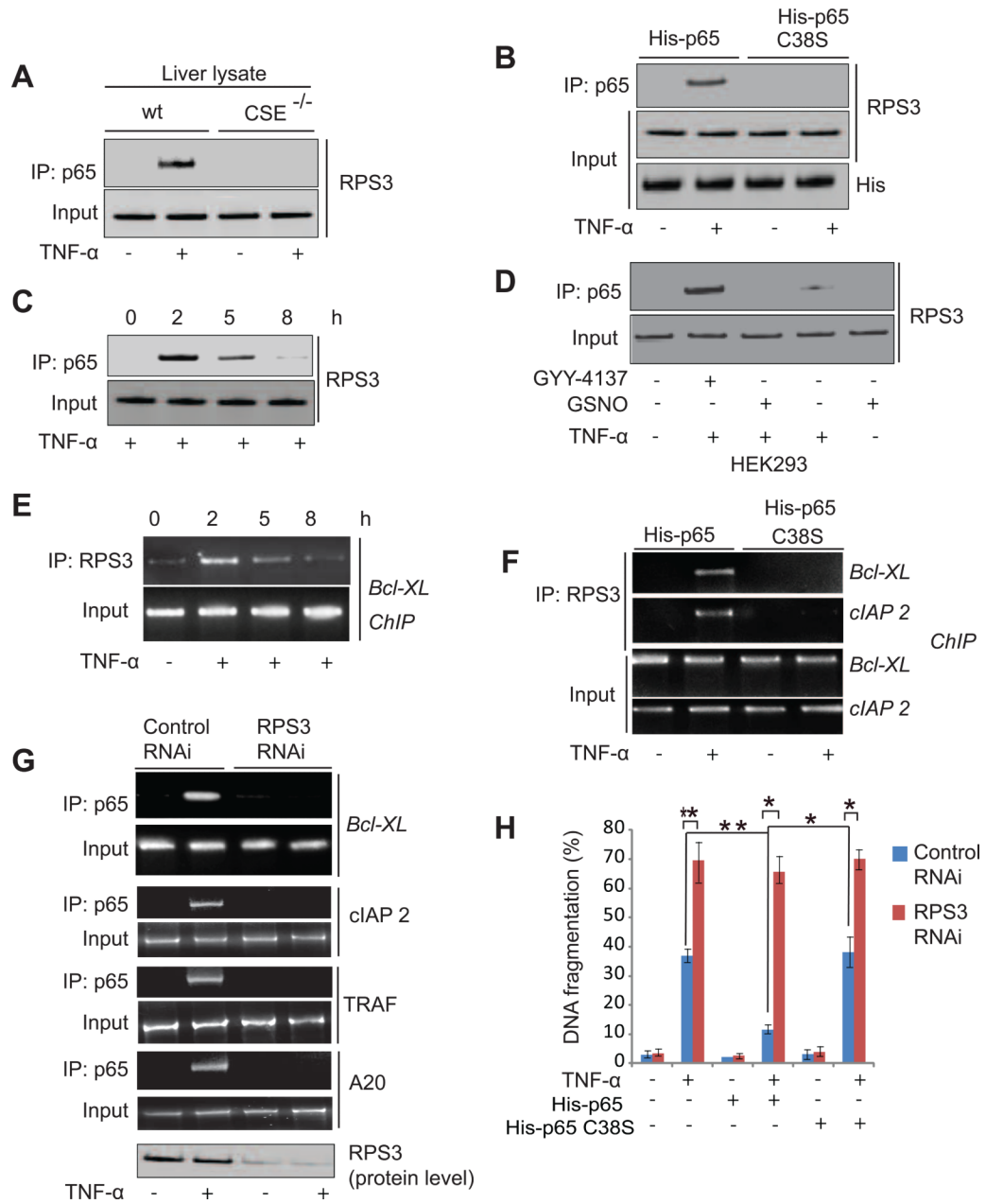
Figure 5. Binding of sulfhydrated p65 to RPS3 is required for transcriptional activity of NF-κB
(**A**) Treatment with TNF-α enhances binding between p65 and RPS3 in liver of wild type but not CSE$^{-/-}$ mice. (**B**) TNF-α elicits binding between RPS3 and wt p65 but not p65-C38S. (**C**) TNF-α elicits binding between p65 and RPS3 in peritoneal macrophages. (**D**) H$_2$S donor GYY-4137 augments p65-RPS3 binding selectively in the presence of. TNF-α but GSNO does not. (**E**) Formation of p65–RPS3 complex at the Bcl-XL promoter region in RAW264.7 cells. (**F**) TNF-α elicits a complex of RPS3 at the Bcl-XL promoter region with p65 but not p65-C38S. (**G**) Depletion of RPS3 abolishes binding of p65 to promoters of the anti-apoptotic genes Bcl-XL, c-IAP2, TRAF and A20. (**H**) Apoptotic effects of TNF-α in macrophages are prevented by overexpression of wt p65. DNA fragmentation is elevated in RPS3 depleted cells. Overexpression of wt p65 does not reverse cell death in RPS3 depleted

cells. *p < 0.01, n = 5, one-way ANOVA, mean ± SEM. **p < 0.001, n = 5, one-way ANOVA, mean ± SEM.